Journal of Nuclear Materials 389 (2009) 45–51

Contents lists available at ScienceDirect

Journal of Nuclear Materials

journal homepage: www.elsevier.com/locate/jnucmat

Thermophysical properties of NpO_2, AmO_2 and CmO_2

V. Sobolev *

Belgian Nuclear Research Centre SCK·CEN, Boeretang 200, BE-2400, Mol, Belgium

ARTICLE INFO

PACS:
65.40.Ba
65.40.De
66.70.+f

ABSTRACT

The information on thermal and mechanical properties of the minor actinide dioxides: NpO_2, AmO_2 and CmO_2, is still very scarce, and a large uncertainty exists because of difficulties related to their fabrication and manipulation. Prognosis based on a set of the sound physical models and the similarity principle can be useful in this situation. Using the combination of the macroscopic and microscopic approaches developed earlier for thermodynamic properties of actinide dioxides, and the Klemmens model for their thermal conductivity, a few relationships bounding the main thermophysical properties of the actinide dioxides were deduced. These relationships were applied for the calculation of the isochoric and isobaric heat capacity, the isobaric thermal expansion coefficient, the isothermal bulk elastic modulus and the thermal conductivity of NpO_2, AmO_2 and CmO_2 in a large temperature range. A rather satisfactory agreement with the available experimental data and recommendations was demonstrated.

1. Introduction

The minor actinides (MA: Np, Am, Cm) accumulated in the nuclear spent fuel are considered as the most important part of the long-life radioactive waste. Their burning in new generation nuclear reactors is proposed to reduce the needed volume for the waste definitive disposal [1]. In this strategy, the design and fabrication of fuels dedicated to MA transmutation are the problems of the highest priority. In the European Roadmap for MA transmutation the dedicated oxide fuels are considered as the main candidates [2]. A large experience was accumulated on the mixed uranium–plutonium oxide fuels, however, the database of thermal and mechanical properties of the MA oxides is still very scarce, and a large uncertainty exists because of the difficulties related to their fabrication and manipulation caused by high radiation levels. This restrains the dedicated fuel design and the prognosis of its operational behaviour. Different sophisticated techniques have been developed and used by different teams for the estimation of the thermomechanical properties of the actinide oxides. During the last years, the molecular dynamic (MD) modelling is intensively used to fill in the empty rooms in the MA-fuel properties database [3,4]. However, this technique cannot yet be used in the fuel performance and design codes. A combined simplified, but adequate physical modelling of the main thermophysical properties of the dedicated fuels, based on the combination of the thermodynamic and microscopic approaches, can be very efficient in this case.

In the present article, the approach presented in [5] is applied to the MA dioxides: NpO_2, AmO_2, and CmO_2. The next chapter gives an expression for the Helmholtz free energy of the MA dioxides and the simplified models of their phonon spectrum and localised electronic excitations. The formulae for calculation of the specific heat, the bulk elastic modulus, the coefficient of thermal expansion and the thermal conductivity are deduced in Chapter 3. In the forth chapter, these formulae are used for prediction of the thermophysical properties of NpO_2, AmO_2, and CmO_2. The obtained results are compared with the experimental data, the published results of MD calculations and the recommendations found in open literature.

2. Free energy of actinide dioxides

The Helmholtz free energy of a solid (F) presented as a function of volume (V) and temperature (T), is a sum of the solid free energy at temperature $T = 0$ K (F_0), the free energy of the crystal lattice thermal excitations (phonons) (F_{ph}), and the energy of the electronic excitations (F_e):

$$F(V,T) = F_0(V) + F_{ph}(V,T) + F_e(V,T). \quad (1)$$

For the oxides of interest, the first term on the right hand side of Eq. (1) consists of the potential energy of the static solid, the ground state energy of the lattice vibrations and the ground state energy of electrons. The volume dependence of the ground state free energy of a solid with volume V can be deduced from the thermodynamic equation of state proposed by Kumar [6]:

* Corresponding author. Tel.: +32 14 33 22 67; fax: +32 14 32 12 16.
E-mail address: vsobolev@sckcen.be

0022-3115/$ - see front matter © 2009 Elsevier B.V. All rights reserved.
doi:10.1016/j.jnucmat.2009.01.005

$$E_0(V) = E_0(V_0) + \frac{V_0 \cdot B_{T0}}{\left(1+\frac{\partial B_{T0}}{\partial p}\right)^2} \cdot \left\{ \left(1+\frac{\partial B_{T0}}{\partial p}\right) \cdot \left(\frac{V}{V_0}-1\right) + e^{\left(1+\frac{\partial B_{T0}}{\partial p}\right)\cdot\left(1-\frac{V}{V_0}\right)} - 1 \right\}, \quad (2)$$

where E_0 is a constant; B_{T0}, the bulk elastic modulus of the solid at $T = 0$ K and p, the external pressure.

The second term in Eq. (1) can be described using the quasi-harmonic approximation for the ideal solid lattice vibrations with the phonon frequencies dependant on volume [7]:

$$F_{ph}(V,T) = 3N \cdot k_B \cdot T \sum_i \int_{\omega_{0i}(V)}^{\omega_{\max i}(V)} \ln\left(1 - e^{\frac{\hbar\cdot\omega}{k_B\cdot T}}\right) \cdot f_i(\omega) \cdot d\omega, \quad (3)$$

where k_B and $\hbar$ are the Boltzmann and Planck constants respectively; N, a number of atoms in the volume V; ω, the phonon angular frequency; $f(\omega)$, the phonon spectral function (density-of-states); i, the index of the phonon branch.

The phonon spectrum of the dioxides of interest, which have fluorite crystal lattice, contains three acoustic translational vibration branches (one with the longitudinal polarisation and two with the transverse polarisations) and six internal optical branches [8]. Taking into account the difficulties in determination of the phonon spectrum, the complexity of the spectrum itself and a small effect of its fine structure on the thermophysical properties, simplified spectrum models are usually used for estimation of the material properties. In our previous publication [5], a simple model of the actinide dioxides phonon spectrum has been proposed where the three acoustic branches were represented by the Debye model: one longitudinal with the characteristic frequency ω_{AL} and one twice degenerated, transversal with the characteristic frequency ω_{AT}, and the six optic branches were condensed into two branches: one twice degenerated, longitudinal and one four times degenerated, transversal. Each optic branch was described with the rectangular parallelepiped-wise function with the lower and upper frequency limits $\omega_{OL\ min}$ and $\omega_{OL\ max}$ for the longitudinal branch and $\omega_{OT\ min}$ and $\omega_{OT\ max}$ for the transverse branch. Then, the normalised (to unity) phonon distribution function of the actinide dioxides is presented as follows:

$$f_{ph}(\omega) = \frac{\omega^2 \cdot H(\omega_{AL}-\omega)}{3\omega_{AL}^3} + \frac{2\omega^2 \cdot H(\omega_{AT}-\omega)}{3\omega_{AT}^3} + \frac{2}{9}\cdot\frac{H(\omega-\omega_{OL\min}) - H(\omega-\omega_{OL\max})}{(\omega_{OL\max}-\omega_{OL\min})} + \frac{4}{9}\cdot\frac{H(\omega-\omega_{OT\min}) - H(\omega-\omega_{OT\max})}{(\omega_{OT\max}-\omega_{OT\min})}. \quad (4)$$

$H(x)$ is the standard unit step Heviside function. The characteristic frequencies of the acoustic branches (ω_{AL} and ω_{AT}) are determined by the longitudinal and transverse components of sound velocity (u_L and u_T) and by a distance between the centres of the neighbour primitive cells of the crystal lattice

$$\omega_{AL} = \frac{\pi\sqrt{2}\cdot u_L}{a} \text{ and } \omega_{AT} = \frac{\pi\sqrt{2}\cdot u_T}{a}, \quad (5)$$

where a is the lattice parameter. The longitudinal and transversal sound velocities are expressed through the bulk elastic modulus, the Poisson ratio (μ) and the density (ρ) [9]

$$u_L = \sqrt{\frac{3B_{T0}\cdot(1-\mu)}{\rho\cdot(1+\mu)}} \text{ and } u_T = \sqrt{\frac{3B_{T0}\cdot(1-2\cdot\mu)}{2\rho\cdot(1+\mu)}}. \quad (6)$$

The maximum and minimum characteristic frequencies of the optic branches are determined using the respective frequency ratios of UO_2 [8], based on the similarity principle.

For insulators, such as the considered dioxides at temperatures higher than 50 K and lower than 2000 K, the temperature dependent part of the electronic component of the Helmholtz potential, the third term in Eq. (1), can either be neglected or determined by the excitations of the unpaired localised 5f electrons. For the actinide dioxides it can be presented as follows [10]:

$$F_e(V,T) = -\frac{N\cdot k_B\cdot T}{3}\cdot\ln\left(\sum_j g_j \cdot e^{-\frac{\Delta E_{ej}(V)}{k_B\cdot T}}\right), \quad (7)$$

where ΔE_{ej} is the electron excitation energy at the jth level; g_j, the degeneracy of the jth level. The parameters of the localised 5f-electron levels of NpO_2, AmO_2, and CmO_2 can be found in [11].

3. Main thermophysical properties

The main thermodynamic parameters of the considered oxides, such as the isothermal bulk modulus (B_T), the isobaric volumetric coefficient of thermal expansion (α_p), the isochoric and isobaric heat capacities (C_V and C_p), can be deduced from their free energy [12]

$$C_V(T,V) = -T\left(\frac{\partial^2 F(T,V)}{\partial T^2}\right)_V, \quad (8)$$

$$B_T(T,V) = V\cdot\left(\frac{\partial^2 F(T,V)}{\partial V^2}\right)_T, \quad (9)$$

$$\alpha_p(T,V) = -\frac{1}{B_T(V,T)}\cdot\left(\frac{\partial}{\partial T}\left(\frac{\partial F(T,V)}{\partial V}\right)_T\right)_V, \quad (10)$$

The actinide dioxide thermal conductivity (κ) is mainly determined by the phonon system (the electronic component is negligible in the considered temperature region of 50–2000 K). It is defined by the kinetic theory of transport phenomena as follows [13]:

$$\kappa(T) = \frac{1}{3\cdot V}\sum_i \int C_{v\,i}(\omega)\cdot u_i(\omega)\cdot l_i(\omega)\cdot d\omega, \quad (11)$$

where $C_{vi}(\omega)\cdot d\omega$ is the contribution of the ith branch phonons with frequencies between ω and $\omega + d\omega$ into the isochoric heat capacity; u_i, the group velocity of the ith branch phonons and l_i, their free path length determined by interactions with static and dynamic defects in the considered solid.

3.1. Heat capacity

The double differentiation of Eq. (1) over the temperature, with the terms determined by (2), (3) and (7) and the phonon spectrum (4), yields the isochoric heat capacity

$$C_V(V,T) = \frac{k_B\cdot N}{3}\cdot\left[D'_3(\theta_{AL}(V)/T) + 2D'_3(\theta_{AT}(V)/T) + 2\cdot\frac{\theta_{OL\max}(V)\cdot D'_1(\theta_{OL\max}(V)/T) - \theta_{OL\min}(V)\cdot D'_1(\theta_{OL\min}/T)}{\theta_{OL\max}(V)-\theta_{OL\min}(V)} + 4\cdot\frac{\theta_{OT\max}(V)\cdot D'_1(\theta_{OT\max}(V)/T) - \theta_{OT\min}(V)\cdot D'_1(\theta_{OT\min}/T)}{\theta_{OT\max}(V)-\theta_{OT\min}(V)} + \sum_j g_j\cdot\left(\frac{\theta_{ej}(V)}{T}\right)^2\cdot\frac{e^{\theta_{ej}(V)/T}}{\left(e^{\theta_{ej}(V)/T}-1\right)^2}\right], \quad (12)$$

where $\theta_i(V) \equiv \hbar\cdot\omega_i(V)/k_B$ and $\theta_{ej}(V) \equiv \Delta E_{ej}(V)/k_B$ are the characteristic temperatures of phonons and electronic excitations and $D'_n(y)$ is the tabulated 2nd kind Debye integral normalised to unity

$$D'_n(y) = n\cdot y^{-n}\cdot\int_0^y x^{n+1}\cdot exp(x)\cdot[exp(x)-1]^{-2}dx. \quad (13)$$

The isobaric heat capacity (C_p) can be expressed through C_V, α_p and B_T as follows [12]:

$$C_p(T,V) = C_V(T,V) + \alpha_p^2(T,V)\cdot B_T(T,V)\cdot V\cdot T. \quad (14)$$

3.2. Thermal expansion coefficient

Assuming that the spectrum of electronic excitations is independent of temperature and pressure, the thermal expansion of solids is determined by anharmonicity of the phonons only. This anharmonicity is presented as volume dependence of the phonon characteristic frequencies or temperatures, and is quantitatively characterised by the Grüneisen parameters (γ_{Gi}) of the phonon branches

$$\gamma_{Gi} \equiv -\partial(\ln\langle\omega_i(V)\rangle)/\partial(\ln V) = -\partial(\ln\theta_i(V))/\partial(\ln V). \quad (15)$$

Using this definition and substituting Eq. (1) in Eq. (10), the isobaric volumetric thermal expansion coefficient can be presented as follows:

$$\alpha_p(V,T) = \frac{1}{B_T(V,T)\cdot V}\cdot\sum_i \gamma_{Gi}\cdot C_{Vi}(V,T), \quad (16)$$

where $C_{Vi}(V,T)$ is the isochoric heat capacity of the ith phonon branch. The determination of γ_{Gi} is rather complicated, therefore in practice Eq. (16) is replaced by

$$\alpha_p(V,T) = \frac{\gamma_G\cdot C_V(V,T)}{B_T(V,T)\cdot V}, \quad (17)$$

where the Grüneisen bulk constant γ_G is often considered as a fitting parameter.

3.3. Bulk modulus

Assuming that the volume dependence of the free energy is the same as the dependence of the ground state energy, the expression for the isothermal bulk modulus can be obtained by insertion of Eq. (2) into Eq. (9):

$$B_T(V,T) \approx \frac{B_{T0}\cdot V\cdot e^{\left(1+\frac{\partial B_{T0}}{\partial p}\right)\cdot\left(1-\frac{V}{V_0}\right)}}{V_0}, \quad (18)$$

B_{T0} and its pressure derivative are assumed to be known (from experiments or estimated with *ab initio* or other theoretical methods). The temperature dependence of B_T is included in Eq. (18) implicitly through the temperature dependence of volume at given pressure, which can be expressed through the isobaric thermal expansion coefficient as follows:

$$V(T) = V_0\cdot e^{\int_0^T \alpha_p(T)dT} \quad (19)$$

3.4. Thermal conductivity

Heat transfer in the oxides of interest is mostly determined by the phonon mechanism. The localised electronic excitations do not contribute to the heat transfer. The contribution of other mechanisms (charge carriers, photons and vacancies) is limited to only a few percents in the considered temperature range (50–2000 K), therefore, they are disregarded in this work. Also the impact of defects on the phonon spectrum (4) is neglected. The acoustic phonon velocities are constant and those of the optic phonons are zero in the used model. With the above postulated assumptions Eq. (11) permits to obtain the following formula for the thermal conductivity of the MA dioxides:

$$\kappa(T) \approx \frac{k_B\cdot N}{9\cdot V}\cdot\left(u_{AL}\cdot\left(\frac{T}{\theta_{AL}}\right)^3\cdot\int_0^{\theta_{AL}/T}\frac{l_{AL}(x)\cdot x^4\cdot e^x\cdot dx}{(e^x-1)^2} + 2\cdot u_{AT}\cdot\left(\frac{T}{\theta_{AT}}\right)^3\cdot\int_0^{\theta_{AT}/T}\frac{l_{AT}(x)\cdot x^4\cdot e^x\cdot dx}{(e^x-1)^2}\right). \quad (20)$$

In order to evaluate the acoustic phonon free path lengths (l_{AL} and l_{AT}), the phonon scattering by the crystalline grain boundaries (l_{gb}), by point defects (l_{pd}) and by other phonons (l_{ph}) was considered, and the linear superposition of the phonon scattering mechanisms was assumed [14]

$$\frac{1}{l(\omega)} = \frac{1}{l_{gb}(\omega)} + \frac{1}{l_{pd}(\omega)} + \frac{1}{l_{ph}(\omega)}. \quad (21)$$

The hypothesis of Casimir was applied for l_{gb}, claiming that it is independent of frequency and equals to the effective crystallite size [13]. This parameter is assumed to be known.

The phonon scattering on the point defects were estimated with the Klemens type formula [15] allowing to express l_{pd} as follows:

$$l_{pd}(\omega) = a_{pd}\cdot\left(\frac{\omega_{max}}{\omega}\right)^4. \quad (22)$$

The parameter a_{pd} depends on the point defect concentration, the lattice constants, elastic and thermal properties of the considered solid [16]; in the present work, it was estimated from the experimental data on thermal conductivity of samples at the lowest temperature.

In materials with the high concentration of the static defects (as actinide dioxides), the contribution of the normal phonon–phonon scattering (*N*-processes) can be neglected in comparison with other scattering mechanisms. The phonon free path length related to the inelastic phonon–phonon scattering ('Umklapp' or *U*-processes) decreases with temperature and with the phonon frequency. It should be inversely proportional to the number of phonons, which can participate in *U*-processes at the given temperature. At high temperatures it is proportional to $\sim T^{-1}\omega^{-2}$ [14]. Therefore, it is proposed to use for $l_{ph}(\omega)$ the following relationship:

$$l_{ph}(\omega) = a_{ph}\cdot(e^{\bar{\theta}/b_U T} - 1)\cdot\frac{\omega_{max}^2}{\omega^2} \quad (23)$$

where a_{ph} and b_U are the constant parameters. The coefficient a_{ph} can be estimated using the modified by Slack [14] formula (proposed earlier by Leibfried-Schlömann) for the intrinsic thermal conductivity of Debye type solids at high temperatures. The application of the Slack's formula and the relation (23) to the considered model of dioxides yields the following equation:

$$\frac{a_U}{b_U} = 8.62\times10^{-26}\cdot\frac{k_B}{h^2}\cdot\frac{a^3\cdot\bar{M}\cdot\bar{\theta}}{\gamma_G^2} \quad (24)$$

where $\bar{M}$ is the mean atomic mass and $\bar{\theta}$ is the mean characteristic temperature of the acoustic phonons. The constant b_U takes into account the fraction of the phonons that can participate in the *U*-processes; $b_U = 4$ was adopted for the considered MA dioxides.

Finally, the substitution of (21)–(24) into Eq. (20) allows to calculate $\kappa(T)$.

4. Results of modelling

The calculation of the heat capacity, the thermal expansion coefficient and the thermal conductivity of NpO_2, AmO_2 and CmO_2 with the above presented formulae requires the following input information: the mass numbers, the lattice parameters, the elastic moduli, the Grüneisen parameters, the electronic excitations spectra, the concentrations and dimensions of the static defects. The lattice parameters have been extracted from the review of Taylor [17]. The results of measurements of the isothermal bulk elastic modulus of NpO_2 and its first derivative over pressure were published by Benedict et al. [18]. The bulk elastic moduli of AmO_2 and CmO_2 were taken from the publication of Li et al. [19]. The Poisson's ratio was assumed to be 0.333 for all three materials.

The spectra of the localised 5f-electron excitations in NpO_2, AmO_2 and CmO_2 were recommended by Konings [11].

The characteristic temperatures of the acoustic phonon branches were found using Eq. (5) and (6). For the minimum and maximum characteristic temperatures (frequencies) of the optical phonon branches, the assumption was made that their ratios to the acoustic frequencies are the same as in UO_2 [8] and the following approximate values were adopted: $\theta_{OLmin} \approx \theta_{AL}$, $\theta_{OLmax} \approx 3\theta_{OLmin}$, $\theta_{OTmin} \approx 1.2\theta_{OLmin}$, $\theta_{OTmax} \approx 2\theta_{OTmin}$. The bulk Gruneisen parameter was considered as a weak fitting parameter with a value close to 2. The above mentioned input parameters used in calculations are presented in Table 1. The phonon free path length limited by static defects was estimated by fitting to the available experimental data on the thermal conductivity at the lowest temperature.

Table 1
Input parameters of the MA dioxides used in calculations [11,17–19].

		NpO_2	AmO_2	CmO_2
Molecular mass (M)	g mol^{-1}	269.047	275.060	279.062
Lattice parameter (a_0)	10^{-10} m	5.4317	5.3735	5.3576
Isothermal bulk modulus (B_{T0})	10^{11} Pa	2.00	2.16	2.18
Pressure derivative of the bulk modulus (B'_T)	–	3.8	3.1	3.1
Poisson's ratio	–	(0.333)	(0.333)	(0.333)
Levels of the localised 5f electrons				
$g_1 \times \Delta E_{e1}$	meV	4×9.2	4×6.5	–
$g_2 \times \Delta E_{e2}$	meV	2×40.5	–	–
Phonon characteristic temperatures				
Acoustic longitudinal (θ_{AL})	K	323	340	339
Acoustic transversal (θ_{AT})	K	162	170	169
Optic longitudinal (θ_{OL})	K	323–970	340–1020	339–1016
Optic transversal (θ_{OT})	K	388–776	408–816	406–812
Grüneisen parameter	–	(1.80)	(1.95)	(2.00)

4.1. Neptunium dioxide

The results of calculation of the isobaric molar heat capacity, the isobaric volumetric coefficient of thermal expansion, the isothermal bulk elastic modulus and the thermal conductivity of NpO_2 together with the available literature data are presented in Fig. 1(a)–(d).

For the heat capacity (Fig. 1(a)), a rather good agreement with the experimental data of Westrum et al. [20] was obtained at low temperatures (30–300 K) and with the results of Serizawa [21] and Nishi et al. [22] at middle (300–1400 K) temperatures. A lack of the data at $T > 1400$ K restricted a comparison for higher temperatures. The MD modelling of the NpO_2 crystal performed by Kurosaki et al. [3,4] shows good results at $T = 700 - 1000$ K, but underestimates the NpO_2 heat capacity al low temperatures (<600 K) and overestimates it at high temperatures (>1200 K).

For the thermal expansion of NpO_2, the experimental results were found only in the temperature range of 298–1600 K [21,23,24]. All sources communicate the results of measurements of the lattice parameter as a function of temperature. These results were converted into the volumetric coefficient of thermal expansion and compared with the result obtained with the proposed model (Fig. 1(b)). A satisfactory agreement was obtained in the temperature range of 400–1600 K. The difference in the region of 298–400 K could be explained by a very large uncertainty appeared during the conversion of the experimental data on the thermal strain into the thermal expansion coefficient (caused by the limited experimental accuracy). As in the case of the heat capacity, the MD modelling [4] underestimates the thermal expansion coefficient at low temperatures ($T < 700$ K).

The isothermal bulk modulus of NpO_2 as function of temperature is presented in Fig 1(c). The experimental results were only found in [18] at one temperature; the value $B_{T0} = 200$ GPa was used as one of the input parameters in the presented model. The MD

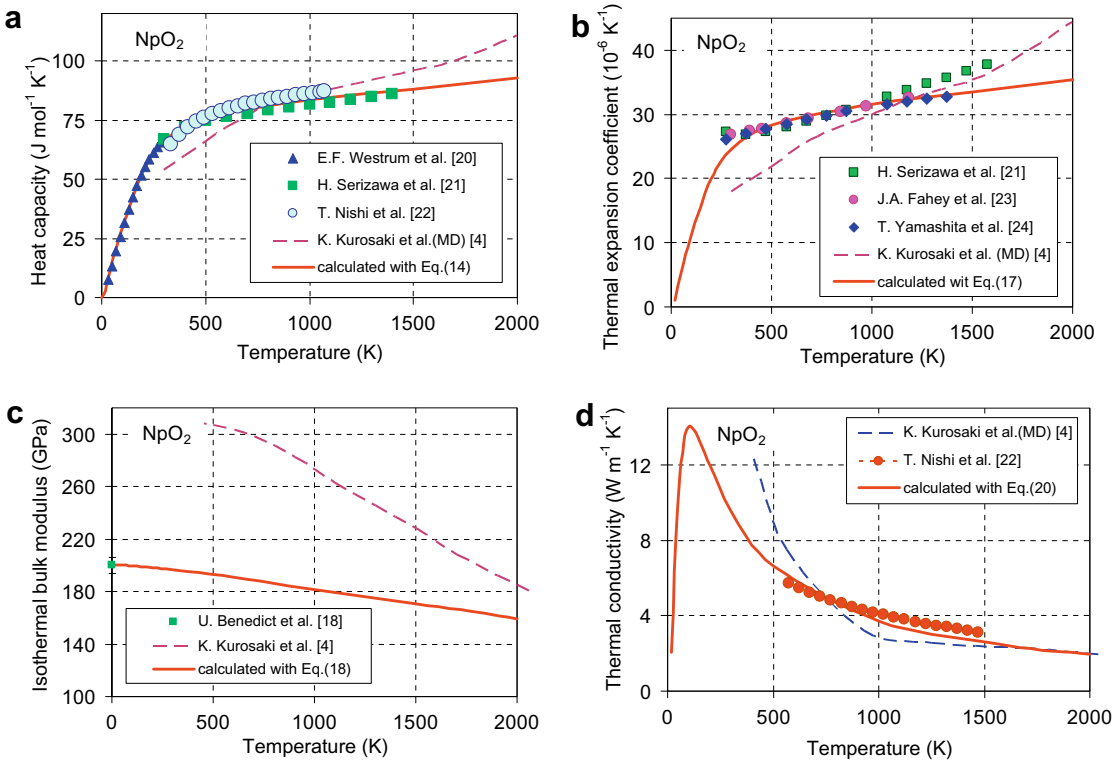

Fig. 1. Calculated and experimental values of the isobaric heat capacity (a), the isobaric volumetric thermal expansion coefficient (b), the isothermal bulk elastic modulus (c) and the thermal conductivity (d) of NpO_2 (normalised to 100% TD).

modelling performed in [3] yields significantly higher values of B_T at low temperatures.

The unique results of measurement of the neptunium dioxide thermal conductivity were published in open literature by Nishi et al. only in 2008 [22]. The results of the thermal conductivity modelling obtained with MD tools were presented few years earlier by Kurosaki et al. [3,4]. Both, together with the results calculated with the proposed model, are presented in Fig. 1(d) for the material of the theoretical density. A rather satisfactory agreement of all results can be seen at temperatures higher than 600 K. At lower temperatures, the MD model [4] overestimates the thermal conductivity because of neglecting the scattering on the static defects.

4.2. Americium dioxide

The calculated heat capacity of AmO_2 was compared with the recommendations of Thiriet and Konings [25] and with the values obtained from the temperature dependence of the AmO_2 enthalpy recommended by Mignanelli and Thetford [26]. A rather good agreement was obtained with the results of [25] in the region of 300–1600 K (Fig. 2(a)). The enthalpy recommendations given in [26] provide the coherent heat capacity value at room temperature but lead to ~10% higher values at $T > 500$ K.

Only one open publication was found with the results of measurement of the AmO_2 thermal expansion [23] at $T = 300$–1100 K. At 300–350 K it provides 10–15% higher values than those calculated with the model, however, rather good agreement was observed in the range of 400–1100 K. The MD results [3] show the same tendency as in the case of NpO_2: underestimation at low temperatures and overestimation at high temperatures.

The situation with the isothermal bulk modulus of AmO_2 is about the same as with that of NpO_2 (see Fig. 2(c)). The recommended in [19] value of $B_{T0} = 216$ GPa was used as one of the input parameters in the model. The MD modelling performed in [3] yields significantly higher B_T at low temperatures.

The thermal conductivity of AmO_{2-x} was measured recently by Nishi et al. [27]. These results together with the data of Bakker and Konings [28], published about ten years earlier, and the results of MD modelling obtained by Kurosaki et al. [3] are presented in Fig. 2(d) (for the material of the theoretical density). The thermal conductivity dependence provided by the present model lies close to both [27] and [28] experimental data sets. The MD modelling [3] shows overestimation at low temperatures (<600 K).

4.3. Curium dioxide

The recommended in [29] and calculated with the enthalpy recommendations of [26] heat capacities of CmO_2 in the temperature range of 300–650 K are presented in Fig. 3(a). The results obtained with the current model are 15–20% below them at $T = 650$ K.

Only two publications on the thermal expansion of curium oxides were found [30,31]. The mean value of 8.1×10^{-6} K^{-1} over the temperature range of 300–650 K was given for the linear coefficient of thermal expansion of CmO_2 in [30]. In [31], a linear increase of the thermal expansion coefficient with temperature was indicated. These results, converted into the isobaric volumetric thermal expansion coefficient, are presented in Fig. 3(b). The self-irradiation defects related to α-decay of curium could be the most probable reason of the observed differences.

The recommendation for the isothermal bulk modulus of CmO_2 was only found in [19]. The recommended value $B_{T0} = 218$ GPa was used as the input parameter (Table 1). The calculated temperature dependence of B_T is presented in Fig. 3(c).

The thermal conductivity of CmO_2 has not yet been well measured, mainly because of the difficulties in the preparation of the high quality CmO_2 samples and in their manipulation. Only one publication [29] was found in open literature with approximate

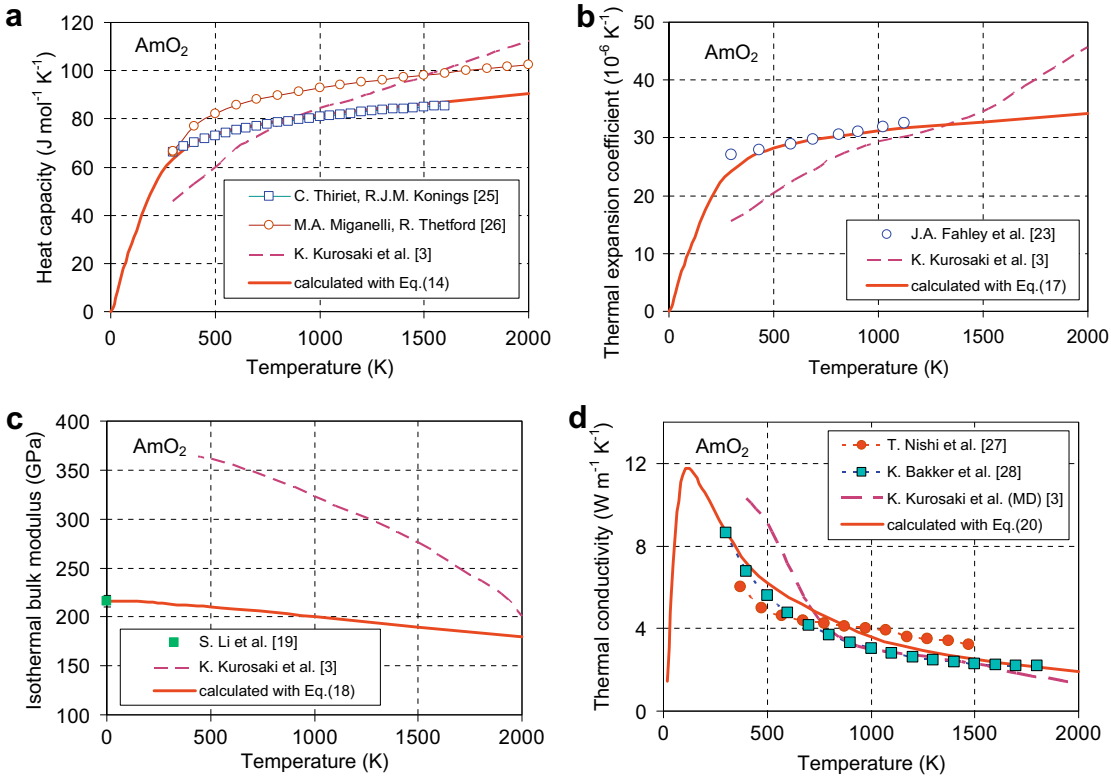

Fig. 2. Calculated and experimental values of the isobaric heat capacity (a), the isobaric volumetric thermal expansion coefficient (b), the isothermal bulk elastic modulus (c) and the thermal conductivity (d) of AmO_2 (normalised to 100% TD).

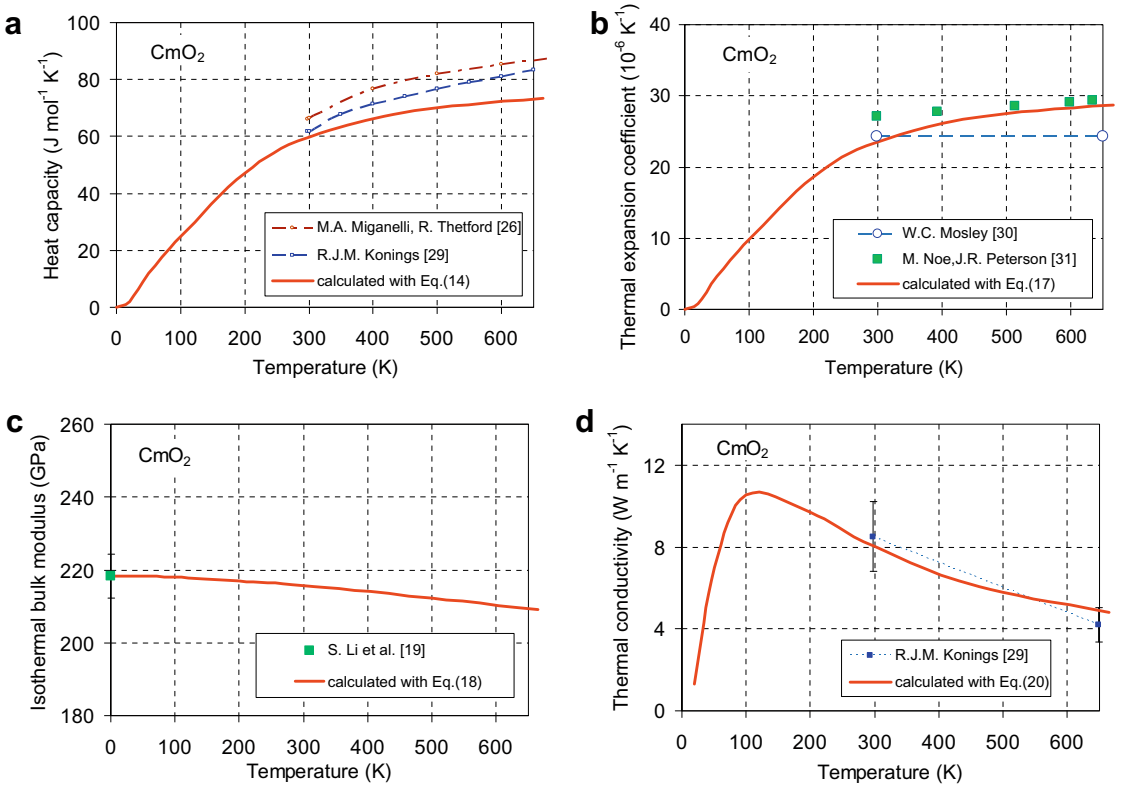

Fig. 3. Calculated and experimental values of the isobaric heat capacity (a), of the isobaric volumetric thermal expansion coefficient (b), the isothermal bulk elastic modulus (c) and of the thermal conductivity (d) of CmO_2 (normalised to 100% TD).

estimations: $\kappa_{CmO_2} = 7–10\ W\ m^{-1}\ K^{-1}$ at $T = 300$ K and $\kappa_{CmO_2} = 3.8–4.6\ W\ m^{-1}\ K^{-1}$ at $T = 650$ K. The calculated temperature dependence of the CmO_2 thermal conductivity fitted to these values is presented in Fig. 3(d).

5. Conclusions

In the frameworks of studies of thermal and mechanical performances of oxide fuels dedicated to the MA transmutation, a set of analytical models was proposed for the calculation of the main thermophysical properties of the actinide dioxides in a large temperature range. The models are based on the simplified phonon spectrum, the quasi-harmonic approximation for the lattice vibrations, and the Klemens approach for the thermal conductivity. The models were applied for the calculation of the isochoric and isobaric heat capacities, the isobaric volumetric thermal expansion coefficient, the isothermal bulk elastic modulus and the thermal conductivity of the minor actinide dioxides: NpO_2, AmO_2, and CmO_2. The comparison of the results of calculations with the available experimental data and recommendations showed a good agreement for NpO_2 and AmO_2. Some underestimation of the thermal expansion should still be explained for CmO_2. Lack of experimental data on the temperature dependence of the bulk elastic modulus and on the thermal conductivity of CmO_2 did not allow a comparison. The developed methodology can be applied for the prognosis of thermophysical properties of other forms of nuclear fuel for which some data are still unavailable or incomplete.

Acknowledgements

This work was supported by funds of the MYRRHA project of the Belgian nuclear research Centre SCK·CEN and by the integrated project EUROTRANS (DM3 AFTRA) of the EURATOM 6th Framework Programme.

References

[1] Advanced Nuclear Fuel Cycles and Radioactive Waste Management, OECD Report NEA No. 5990, Nuclear Energy Agency, OECD Publications, Paris, 2006.
[2] The Sustainable Nuclear Energy Technology Platform: A vision report, EURATOM Report EUR-22842, Director-General for Research, European Commission, Luxemberg: Office for Official Publications of the European Communities 2007.
[3] K. Kurosaki, M. Imamura, I. Sato, T. Namekawa, M. Uno, Sh. Yamanaka, J. Nucl. Sci. Technol. 41 (2004) 827.
[4] K. Kurosaki, M. Imamura, I. Sato, T. Namekawa, M. Uno, Sh. Yamanaka, J. Alloys Compd. 387 (2005) 9.
[5] V. Sobolev, J. Nucl. Matter. 344 (2005) 198.
[6] M. Kumar, Physica B: Cond. Matter. 212B (1995) 391.
[7] C. Kittel, Introduction to Solid State Physics, 2nd Ed., J. Wiley and Sons Inc., New York, 1956.
[8] G. Dolling, R.A. Cowley, A.D.B. Woods, Canad. J. Phys. 43 (1965) 1397.
[9] W.P. Mason, Physical Acoustics and the Properties of Solids, D. Van Nostrand Comp, Princeton, 1958.
[10] Sh. Peng, G. Grimvall, J. Nucl. Mater. 210 (1994) 115.
[11] R.J.M. Konings, J. Chem, Thermodynamics 36 (2004) 121.
[12] C. Kittel, Thermal Physics, J. Willey and Sons, New York, 1976.
[13] P.G. Klemmens, in: R.P. Tye (Ed.), Thermal Conductivity, Academic Press, New York, 1969, p. 1.
[14] G.A. Slack, in: H. Ehrenreich, F. Seitz, D. Turnbull (Eds.), Solid State Physics, vol. 34, Academic Press, New York, 1979, p. 1.
[15] P.G. Klemmens, in: H. Ehrenreich, F. Seitz, D. Turnbull (Eds.), Solid State Physics, vol. 7, Academic Press, New York, 1959, p. 1.
[16] J.M. Ziman, Electrons and Phonons: The Theory of Transport Phenomena in Solids, Clarendon Press, Oxford, Oxford Classics Series, 2001.
[17] R. Taylor, Brit. Ceram. Trans. J. 83 (1984) 32.
[18] U. Benedict, S. Dabos, C. Dufour, J.C. Spirlet, J. Less-Common Met. 121 (1986) 461.
[19] S. Li, R. Ahuja, B. Johansson, High Press. Res. 22 (2002) 471.
[20] E.F. Westrum, J.B. Hatcher, D.W.J. Osborne, Chem. Phys. 21 (1953) 419.
[21] H. Serizawa, J. Chem, Termodynamics 33 (2001) 615.
[22] T. Nishi, A. Itoh, M. Takano, M. Numata, M. Akabori, Y. Arai, K. Minato, J. Nucl. Mater. 376 (2008) 78.

[23] J.A. Fahey, R.P. Turcotte, T.D. Chikalla, Inorg. Nucl. Chem. Let. 10 (1974) 459.
[24] T. Yamashita, N. Nitani, T. Tsuji, H. Inagaki, J. Nucl. Mater. 247 (1997) 90.
[25] C. Thiriet, R.J.M. Konings, J. Nucl. Mater. 320 (2003) 292.
[26] M.A. Mignanelli, R. Thetford, in: Workshop Proceedings Advanced Reactors with Innovative Fuels (ARWIF–2001), 22–24 October, 2001, Chester, UK, Paper No. 52, OECD, NEA, 2002, p. 161.
[27] T. Nishi, M. Takano, A. Itoh, M. Akabori, Y. Arai, K. Minato, M. Numata, J. Nucl. Mater. 373 (2008) 295.
[28] K. Bakker, R.J.M. Konings, J. Nucl. Mater. 254 (1998) 129.
[29] R.J.M. Konings, J. Nucl. Mater. 298 (2001) 255.
[30] W.C. Mosley, J. Inorg, Nucl. Chem. 34 (1972) 539.
[31] M. Noé, J.R. Peterson, Inorg. Nucl. Chem. Let. 8 (1972) 897.